

# Importance of Itinerancy and Quantum Fluctuations for the Magnetism in Iron Pnictides

Yu-Zhong Zhang<sup>\*a,b</sup>, Hunpyo Lee<sup>a</sup>, Ingo Opahle<sup>a</sup>, Harald O. Jeschke<sup>a</sup>, Roser Valentí<sup>a</sup>

<sup>a</sup>*Institut für Theoretische Physik, Goethe-Universität Frankfurt, Max-von-Laue-Straße 1, 60438 Frankfurt am Main, Germany*

<sup>b</sup>*Department of Physics, Tongji University, Shanghai, 200092 P. R. China*

## Abstract

By applying density functional theory, we find strong evidence for an itinerant nature of magnetism in two families of iron pnictides. Furthermore, by employing dynamical mean field theory with continuous time quantum Monte Carlo as an impurity solver, we observe that the antiferromagnetic metal with small magnetic moment naturally arises out of coupling between unfrustrated and frustrated bands. Our results point to a possible scenario for magnetism in iron pnictides where magnetism originates from a strong instability at the momentum vector  $(\pi, \pi, \pi)$  while it is reduced by quantum fluctuations due to the coupling between weakly and strongly frustrated bands.

## Key words:

Iron pnictides, itinerant magnetism, density functional theory, dynamical mean field theory, multi-band Hubbard model.

PACS: 74.70.Xa, 75.10.-b, 71.15.Mb, 71.10.Fd, 71.30.+h

## 1. Introduction

Since the discovery of high- $T_c$  superconductivity in LaOFeAs [1], great effort has been devoted to pursuing higher superconducting transition temperatures  $T_c$  [2] as well as to the understanding of the various phase transitions in these materials as a function of temperature, pressure and doping [3, 4, 5]. Density functional theory (DFT) calculations [6, 7] show that electron-phonon coupling – though non-negligible – is not strong enough to explain the high  $T_c$  observed in these systems. Instead, magnetically mediated pairing has been proposed to account for the superconducting state due to its proximity to a stripe-type antiferromagnetic (AF) metallic state [8, 9].

However, the origin of the stripe-type AF metal, i.e., whether it comes from the itinerant nature of the Fermi surface (FS) nesting [9, 10, 11, 12, 13] or a localized picture of exchange interactions between local spins [14, 15, 16], is still under debate. The scenario of FS nesting was severely challenged by recent DFT calculations [17], which found a disconnection between Fe moment and FS nesting. However, a recent revision of the nature of magnetism in the iron pnictides – also within DFT, but with more precise optimized structures – has reestablished the close connection between itinerancy and magnetism [13]. In this work, we will present further clear evidence of the itinerant nature of magnetism by performing DFT calculations for a few families of iron pnictides.

On the other hand, the disagreement [18, 19] of the magnitude of the Fe moment in the stripe-type AF metal between experimental observations and DFT calculations based on experimental structures is still controversially discussed. Various mechanisms have been proposed from DFT calculations,

for example, negative effective on-site electronic interaction  $U$  [20, 21], a low moment solution within GGA+ $U$  stabilized by the formation of magnetic multipoles [22, 23] or frustration between local spins [14, 15, 24, 25]. Recently, also mean-field calculations based on a five-band Hubbard model with positive  $U$  obtained a small magnetic moment comparable to experimental results [26, 27, 28]. However, the existence of various sets of DFT-derived hopping parameters [29, 30, 31] casts doubt on the reliability of the model parameters used in the model calculations.

From DFT calculations it is well known [8, 18, 19] that the physical properties of the iron pnictides are highly sensitive to details of the structure as well as to details of the exchange and correlation (XC) functionals. For instance, structural optimization within the local spin density approximation (LSDA) leads to almost perfect agreement [18] with the most recent experimental value of the Fe moment [32]. This indicates, that quantum fluctuations, which are only insufficiently incorporated in the common approximations to DFT, could strongly improve the agreement with experiment.

To further explore this, we employ dynamical mean-field theory (DMFT) [33] combined with continuous time quantum Monte Carlo (CTQMC) [34] simulations. A feature that is common to different sets of DFT-derived hopping parameters is the presence of some strongly and some weakly frustrated Fe  $3d$  bands [29, 30, 31]. In the present work we consider a *minimal* two-band Hubbard model which should capture this feature by considering one band with frustration and the second one without frustration and we investigate the effect of the coupling of these two bands on the magnetism of the system. We would like to remark that while a realistic description of the Fe systems needs at least a five-band model, the present two-band model should be sufficient for the proposed analysis. We find that an

<sup>\*</sup>Corresponding author.

Email address: yzhang@itp.uni-frankfurt.de (Yu-Zhong Zhang)

AF metallic state is present in a wide range of the interaction parameter  $U$  when one band is highly frustrated and the second one unfrustrated, while the state is absent when both bands are equally frustrated [35].

Our results from DFT and DMFT suggest that a strong instability at a momentum vector  $(\pi, \pi, \pi)$  is the promising mechanism for the itinerant magnetism observed in iron pnictides while quantum fluctuations originating from the coupling between weakly and strongly frustrated bands reduce the magnetic moment and make it more comparable to the experimental observations.

## 2. Method and Model

In order to quantify the FS nesting and hence the itinerant nature of the magnetism, we calculate (i) the  $\mathbf{q}$ -dependent Pauli susceptibility at  $\omega=0$  with the constant matrix element approximation, defined as

$$\chi_0(\mathbf{q}) = - \sum_{\mathbf{k}\alpha\beta} \frac{f(\varepsilon_{\mathbf{k}\alpha}) - f(\varepsilon_{\mathbf{k}+\mathbf{q}\beta})}{\varepsilon_{\mathbf{k}\alpha} - \varepsilon_{\mathbf{k}+\mathbf{q}\beta} + i\delta} \quad (1)$$

where  $\alpha$  and  $\beta$  are band indexes and  $q$  and  $k$  are momentum vectors in the Brillouin zone, and (ii) the  $k_z$  dispersion of the FS. These calculations were performed with the full potential linearized augmented plane wave method as implemented in the WIEN2k code [36] with  $RK_{\max} = 7$ . While 40000  $\mathbf{k}$  points are used in calculating the  $k_z$  dispersion of the FS, a three dimensional grid of  $128 \times 128 \times 128$   $\mathbf{k}$  and  $\mathbf{q}$  points are employed for the susceptibility. All calculations were performed in the scalar relativistic approximation.

In order to perform the DFT analysis, (i) we use the available experimental structures for LaOFeAs [37], BaFe<sub>2</sub>As<sub>2</sub> [38] and (ii) we obtain fully optimized structures for BaFe<sub>2-x</sub>Co<sub>x</sub>As<sub>2</sub> within the virtual crystal approximation and for a few hypothetical compounds like LaOFeSb and BaFe<sub>2</sub>Sb<sub>2</sub> using the Car-Parrinello [39] projector-augmented wave [40] method. Our optimized structures compare well with the experimental ones [13, 41]. Part of our results are double-checked by the full potential local orbital (FPLO) method [42]. Results are consistent among these methods. Throughout the paper, the Perdew-Burke-Ernzerhof generalized gradient approximation (GGA) to DFT has been used.

For our model calculations we consider the following two-band Hubbard model

$$H = - \sum_{\langle ij \rangle m \sigma} t_m c_{im\sigma}^\dagger c_{jm\sigma} - \sum_{\langle ij' \rangle m \sigma} t'_m c_{im\sigma}^\dagger c_{j'm\sigma} + U \sum_{im} n_{im\uparrow} n_{im\downarrow} + \sum_{i\sigma\sigma'} (U' - \delta_{\sigma\sigma'} J_z) n_{i1\sigma} n_{i2\sigma'}, \quad (2)$$

where  $t_m$  ( $t'_m$ ) is the intra-band hopping integral between nearest-neighbor (next nearest-neighbor) sites with band indices  $m = 1, 2$ . For simplification, we neglect inter-band hybridizations.  $U$ ,  $U'$  and  $J_z$  are the intra-band, inter-band Coulomb interaction and Ising-type Hund's coupling, respectively. In our calculations we set  $U' = \frac{U}{2}$  and  $J_z = \frac{U}{4}$  which

fulfills the rotational invariance condition of  $U = U' + 2J$  and ignore the spin-flip and pair-hopping processes. The operators are written in the standard notation of the multi-band Hubbard model [35]. In order to solve this model we employ the two-sublattice DMFT method [33] which includes the local quantum fluctuation effects and can account for the AF state, combined with CTQMC simulations [34]. Existing DMFT studies combining with DFT calculations are focused on paramagnetic state [43, 44, 45, 46, 47]. Our calculations are performed on the Bethe lattice.

## 3. Results and Discussion

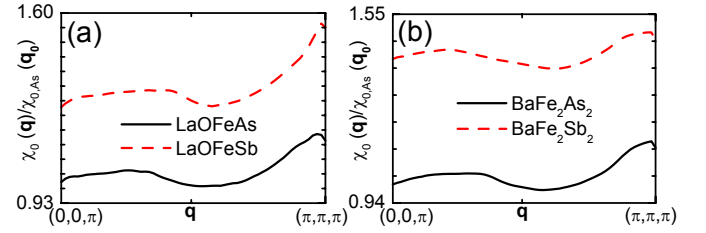


Figure 1: (Color online) Comparison of normalized  $\mathbf{q}$ -dependent Pauli susceptibilities calculated within GGA at fixed  $q_z = \pi$  along the [110] direction between arsenide and antimonide of (a) 1111 compounds and (b) 122 compounds. The normalization factors are the susceptibilities of the corresponding arsenide systems for each type of compound at  $\mathbf{q}_0 = (0, 0, \pi)$ . Please note that the peak position is not exactly at  $\mathbf{q}_\pi = (\pi, \pi, \pi)$  since the electron and hole FSs are nearly nested rather than perfectly nested.

Table 1: Magnetic moment calculated within spin-polarized GGA based on experimental structures of LaOFeAs and BaFe<sub>2</sub>As<sub>2</sub> and optimized structures of the hypothetical compounds LaOFeSb and BaFe<sub>2</sub>Sb<sub>2</sub>.

	LaOFeAs	LaOFeSb	BaFe <sub>2</sub> As <sub>2</sub>	BaFe <sub>2</sub> Sb <sub>2</sub>
$m(\mu_B)$	1.8	2.2	2.0	2.5

In Fig. 1, we present the comparison of  $\mathbf{q}$ -dependent Pauli susceptibilities between arsenide and antimonide 1111 and 122 compounds normalized by the susceptibilities of the corresponding arsenide systems for each type of compound at  $\mathbf{q}_0 = (0, 0, \pi)$ . Here we only consider  $q_z = \pi$  since in both LaOFeAs and BaFe<sub>2</sub>As<sub>2</sub> the Fe spins are AF ordered along  $c$  as experimentally observed and we show the results for  $q_x = q_y$ . We observe that in all these four compounds a strong peak around  $\mathbf{q}_\pi = (\pi, \pi, \pi)$  is found, which supports the presence of stripe-type magnetically ordered states as observed experimentally. Most importantly, in contrast to an earlier DFT study [17] where the magnetic moment increases as As is replaced by Sb in both LaOFeAs and BaFe<sub>2</sub>As<sub>2</sub> while the susceptibilities at  $\mathbf{q}_\pi$  decrease in BaFe<sub>2</sub>Sb<sub>2</sub> compared to BaFe<sub>2</sub>As<sub>2</sub>, which is interpreted to be evidence of disconnection between FS nesting and magnetism, our results show that in both compounds, the susceptibilities at  $\mathbf{q}_\pi$  increase as the replacement takes place and simultaneously the magnetic moment is also enhanced as displayed in Table. 1. This discrepancy is attributed to the improved precision of optimized lattice structures in our DFT cal-

culation [13]. Therefore, the close connection between itinerancy and magnetism remains.

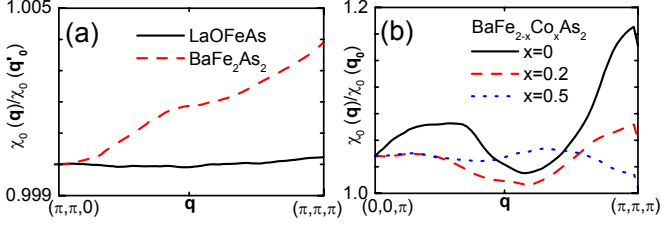


Figure 2: (Color online) (a) Normalized  $\mathbf{q}$ -dependent Pauli susceptibilities of LaOFeAs and BaFe<sub>2</sub>As<sub>2</sub> at fixed  $q_x = q_y = \pi$  along the [001] direction calculated within GGA. The normalization factors are the susceptibilities of each compound at  $\mathbf{q}'_0 = (\pi, \pi, 0)$ , and the experimental structure is used. (b) Normalized  $\mathbf{q}$ -dependent Pauli susceptibilities of BaFe<sub>2-x</sub>Co<sub>x</sub>As<sub>2</sub> at fixed  $q_z = \pi$  along the [110] direction calculated within GGA. Here  $x = 0, 0.2, 0.5$ . The normalization factors are the susceptibilities of each compound at  $\mathbf{q}_0 = (0, 0, \pi)$ .

In Fig. 2 (a), we show the  $\mathbf{q}$ -dependent Pauli susceptibilities of LaOFeAs and BaFe<sub>2</sub>As<sub>2</sub> at fixed  $q_x = \pi$  and  $q_y = \pi$ , normalized by the susceptibilities of each compound at  $\mathbf{q}'_0 = (\pi, \pi, 0)$ . We find that while a tiny increase of the susceptibilities is found from  $\mathbf{q}'_0$  to  $\mathbf{q}_\pi$  in LaOFeAs, indicating a dispersionless FS along  $c$  and therefore nearly perfect two dimensional physical properties, a stronger enhancement is seen in BaFe<sub>2</sub>As<sub>2</sub> suggesting a three dimensional FS topology as shown in Fig. 3 (a), (b), even though it is a layered compound. Such a three dimensionality of the FS has been proposed to be the mechanism for a nearly isotropic critical field in (Ba,K)Fe<sub>2</sub>As<sub>2</sub> [48]. The common feature in the susceptibilities for LaOFeAs and BaFe<sub>2</sub>As<sub>2</sub> is that the values at  $\mathbf{q}_\pi$  are larger than those at  $\mathbf{q}'_0$  which can account for the AF arrangement of Fe spins along  $c$ , although the interlayer interaction is believed to be small. Such a consistency again implies a close relation between itinerancy and magnetism.

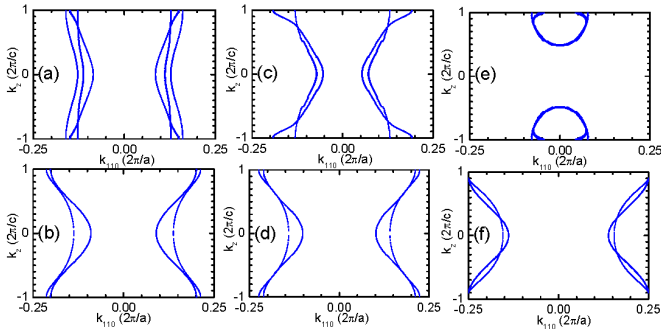


Figure 3: (Color online)  $k_z$  dispersion of FS calculated within GGA as a function of Co-doping in BaFe<sub>2-x</sub>Co<sub>x</sub>As<sub>2</sub> around  $\Gamma$  at  $x = 0$  (a), at  $x = 0.2$  (c), at  $x = 0.5$  (e) and around X at  $x = 0$  (b), at  $x = 0.2$  (d), at  $x = 0.5$  (f).

It has already been shown that changes in the FS topology can explain the different nature of structural and magnetic phase transitions in the 122 compounds under pressure [11, 49]. In the following we will further demonstrate that the phase transitions in BaFe<sub>2</sub>As<sub>2</sub> under Co-doping are also related to the change of FS topology. It is known from experiments [50] that for BaFe<sub>2-x</sub>Co<sub>x</sub>As<sub>2</sub> at  $x = 0$ , the system shows a stripe-type AF

metal. At  $x = 0.2$  the system becomes superconducting, and finally at  $x = 0.5$ , both magnetization and superconductivity disappear. In Fig. 3 we show the  $k_z$  dispersion of the FS for these three cases around  $\Gamma$  (left panels) and X (right panels). We find that the FS along  $c$  becomes more dispersive with Co doping. At  $x = 0$  a strong instability in the Pauli susceptibility – though the FS nesting is not perfect – is present at  $\mathbf{q}_\pi$  as shown in Fig. 2 (b) solid curve, supporting the AF state. At  $x = 0.2$ , the distortion of the FS indicates a strong suppression of the  $\mathbf{q}_\pi$  instability (see Fig. 2 (b) dashed curve) and therefore of the magnetization. However, the superconducting state which, according to the spin fluctuation theory [51], is related to the instabilities around  $\mathbf{q}_\pi$  may in such a situation be more favourable than magnetization. At  $x = 0.5$ , the FS around  $\Gamma$  shrinks to a Fermi pocket and is even more distorted around X, suggesting that no obvious instability in the susceptibility will be present (see Fig. 2 (b) dotted curve) and leading to the disappearance of both magnetic ordering and superconductivity.

After having presented various evidence for the itinerant nature of magnetism in iron pnictides, we will investigate in what follows a possible mechanism for the reduced magnetic moment observed experimentally compared to DFT calculations [11, 18, 19]. As mentioned in Section 1, we would like to extract essential physics from a simplified model as introduced in Section 2. In this model, local quantum fluctuations are included in the calculations by employing DMFT. Fig. 4 shows the magnetization as a function of  $U$  at two temperatures. Combining these results with the analysis of density of states in Ref. [35], we conclude that when two bands are equally highly frustrated (see Fig. 4 (a)), a first-order phase transition from a paramagnetic metal to an AF insulator state is observed and an AF metallic state is absent, while, if one band is unfrustrated and the second one highly frustrated (see Fig. 4 (b)), several continuous phase transitions appear separately in these two bands, and an AF metal with small magnetic moment emerges out of the coupling between highly frustrated and unfrustrated bands, which is the case in iron pnictides as mentioned in Section 1, rather than out of a pure frustration effect.

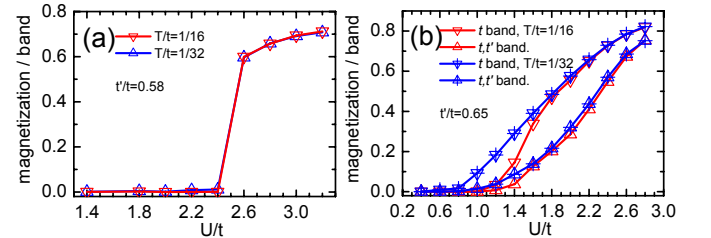


Figure 4: (Color online) Magnetization per band of a two-band Hubbard model at two temperatures calculated by DMFT(CTQMC) as a function of interaction strength  $U$  with (a) two bands equally highly frustrated and (b) one band highly frustrated, the other unfrustrated.

## 4. Conclusion

In summary, we presented various evidence for the close relation between itinerancy and the magnetism observed experimentally. Our results support the itinerant nature of magnetism in iron pnictides and suggest that a strong instability at the nesting vector  $\mathbf{q}_\pi$  is responsible for the magnetism in iron pnictides. We also propose that the reason why the reduced magnetic moment in the iron pnictides cannot be reproduced by LSDA or GGA calculations employing the experimental lattice structure is the insufficient incorporation of quantum fluctuations in such calculations. By applying the DMFT approach to a simplified two-orbital Hubbard model, we propose that coupling of strongly frustrated and unfrustrated bands may be the mechanism for the reduction of the magnetic moment, rather than a pure frustration effect.

We gratefully acknowledge useful discussions and comments from L. Nordström and the Deutsche Forschungsgemeinschaft (DFG) for financial support through SFB/TRR 49, SPP 1458, Emmy Noether programs and the Helmholtz Association for support through HA216/EMMI.

## References

- [1] Y. Kamihara, T. Watanabe, M. Hirano, and H. Hosono, *J. Am. Chem. Soc.* **130**, 3296 (2008).
- [2] Z. A. Ren, W. Lu, J. Yang, W. Yi, X. L. Shen, Z. C. Li, G. C. Che, X. L. Dong, L. L. Sun, F. Zhou, and Z. X. Zhao, *Chin. Phys. Lett.* **25**, 2215 (2008).
- [3] H. Luetkens, H.-H. Klauss, M. Kraken, F. J. Litterst, T. Dellmann, R. Klingeler, C. Hess, R. Khasanov, A. Amato, C. Baines, M. Kosmala, O. J. Schumann, M. Braden, J. Hamann-Borrero, N. Leps, A. Kondrat, G. Behr, J. Werner, B. Büchner, *Nature Materials* **8**, 305 (2009).
- [4] S. A. J. Kimber, A. Kreyssig, Y.-Z. Zhang, H. O. Jeschke, R. Valentí, F. Yokaichiya, E. Colombier, J. Yan, T. C. Hansen, T. Chatterji, R. J. McQueeney, P. C. Canfield, A. I. Goldman and D. N. Argyriou, *Nature Materials* **8**, 471 (2009).
- [5] S. Medvedev, T.M. McQueen, I. Trojan, T. Palasyuk, M.I. Erements, R.J. Cava, S. Naghavi, F. Casper, V. Ksenofontov, G. Wortmann, C. Felser, *Nature Materials* **8**, 630 (2009).
- [6] L. Boeri, O. V. Dolgov, A. A. Golubov, *Phys. Rev. Lett.* **101**, 026403 (2008).
- [7] L. Boeri, M. Calandra, I. I. Mazin, O. V. Dolgov, F. Mauri, *arXiv:1004.1943*.
- [8] D. J. Singh and M.-H. Du, *Phys. Rev. Lett.* **100**, 237003 (2008).
- [9] I. I. Mazin, D. J. Singh, M. D. Johannes and M. H. Du, *Phys. Rev. Lett.* **101**, 057003 (2008).
- [10] V. Cvetkovic and Z. Tesanovic, *Europhys. Lett.* **85**, 37002 (2009).
- [11] Y.-Z. Zhang, H. C. Kandpal, I. Opahle, H. O. Jeschke, and R. Valentí, *Phys. Rev. B* **80**, 094530 (2009).
- [12] A. N. Yaresko, G.-Q. Liu, V. N. Antonov, O.K. Andersen, *Phys. Rev. B* **79**, 144421 (2009).
- [13] Y.-Z. Zhang, I. Opahle, H. O. Jeschke, and R. Valentí, *Phys. Rev. B* **81**, 094505 (2010).
- [14] Q. Si and E. Abrahams, *Phys. Rev. Lett.* **101**, 076401 (2008).
- [15] T. Yildirim, *Phys. Rev. Lett.* **101**, 057010 (2008).
- [16] B. Schmidt, M. Siahatgar, P. Thalmeier, *Phys. Rev. B* **81**, 165101 (2010).
- [17] C.-Y. Moon, S. Y. Park, and H. J. Choi, *Phys. Rev. B* **80**, 054522 (2009).
- [18] I. Opahle, H. C. Kandpal, Y. Zhang, C. Gros, and R. Valentí, *Phys. Rev. B* **79**, 024509 (2009).
- [19] I. I. Mazin, M. D. Johannes, L. Boeri, K. Koepernik, and D. J. Singh, *Phys. Rev. B* **78**, 085104 (2008).
- [20] H. Nakamura, N. Hayashi, N. Nakai, M. Machida, *arXiv:0806.4804*.
- [21] J. Ferber, Y. Z. Zhang, H. O. Jeschke, R. Valentí, *arXiv:1005.1374*.
- [22] F. Cricchio, O. Grånäs, L. Nordström, *Phys. Rev. B* **81**, 140403(R) (2010).
- [23] The stabilized solution with small magnetic moment was found in GGA+U with a positive U and employing the double counting scheme of around mean field. This solution ceases to be favorable when the double counting scheme of fully localized limit is considered.
- [24] F. Ma, Z.-Y. Lu, T. Xiang, *Phys. Rev. B* **78**, 224517 (2008).
- [25] M. J. Han, Q. Yin, W. E. Pickett, and S. Y. Savrasov, *Phys. Rev. Lett.* **102**, 107003 (2009).
- [26] E. Kaneshita, T. Morinari, T. Tohyama, *Phys. Rev. Lett.* **103**, 247202 (2009).
- [27] E. Bascones, M. J. Calderón, and B. Valenzuela, *Phys. Rev. Lett.* **104**, 227201 (2010).
- [28] P. M. R. Brydon, Maria Daghofer, and Carsten Timm, *arXiv:1007.1949v1*.
- [29] T. Miyake, K. Nakamura, R. Arita, M. Imada, *J. Phys. Soc. Jpn.* **79**, 044705 (2010).
- [30] S. Graser, T. A. Maier, P. J. Hirschfeld, D. J. Scalapino, *New J. Phys.* **11**, 025016 (2009).
- [31] K. Kuroki, S. Onari, R. Arita, H. Usui, Y. Tanaka, H. Kontani, and H. Aoki, *Phys. Rev. Lett.* **101**, 087004 (2008).
- [32] N. Qureshi, Y. Drees, J. Werner, S. Wurmehl, C. Hess, R. Klingeler, B. Büchner, M. T. Fernández-Díaz, and M. Braden, *arXiv:1002.4326*.
- [33] A. Georges, G. Kotliar, W. Krauth, M. J. Rozenberg, *Rev. Mod. Phys.* **68**, 13 (1996).
- [34] A. N. Rubtsov, V. V. Savkin, A. I. Lichtenstein, *Phys. Rev. B* **72**, 035122 (2005).
- [35] H. Lee, Y.-Z. Zhang, H. O. Jeschke, and R. Valentí, *Phys. Rev. B* **81**, 220506(R) (2010).
- [36] P. Blaha, K. Schwarz, G. Madsen, D. Kvaniscka, and J. Luitz, *WIEN2K, An Augmented Plane Wave+Local Orbitals Program for Calculating Crystal*, edited by K. Schwarz (Techn. University, Vienna, Austria, 2001).
- [37] T. Nomura, S. W. Kim, Y. Kamihara, M. Hirano, P. V. Sushko, K. Kato, M. Takata, A. L. Shluger, H. Hosono, *Supercond. Sci. Technol.* **21**, 125028 (2008).
- [38] Q. Huang, Y. Qiu, Wei Bao, M. A. Green, J. W. Lynn, Y. C. Gasparovic, T. Wu, G. Wu, and X. H. Chen, *Phys. Rev. Lett.* **101**, 257003 (2008).
- [39] R. Car, M. Parrinello, *Phys. Rev. Lett.* **55**, 2471 (1985).
- [40] P. E. Blöchl, *Phys. Rev. B* **50**, 17953 (1994).
- [41] S. Thirupathaiah, S. de Jong, R. Ovsyannikov, H. A. Dürr, A. Varykhalov, R. Follath, Y. Huang, R. Huisman, M. S. Golden, Yu-Zhong Zhang, H. O. Jeschke, R. Valentí, A. Erb, A. Gloskovskii, and J. Fink, *Phys. Rev. B* **81**, 104512 (2009).
- [42] K. Koepernik and H. Eschrig, *Phys. Rev. B* **59**, 1743 (1999). <http://www.FPLO.de>
- [43] K. Haule, J. H. Shim, G. Kotliar, *Phys. Rev. Lett.* **100**, 226402 (2008).
- [44] L. Craco, M. S. Laad, S. Leoni, H. Rosner, *Phys. Rev. B* **78**, 134511 (2008).
- [45] S. L. Skornyakov, A. V. Efremov, N. A. Skorikov, M. A. Korotin, Yu. A. Izyumov, V. I. Anisimov, A. V. Kozhevnikov, D. Vollhardt, *Phys. Rev. B* **80**, 092501 (2009).
- [46] H. Ishida, A. Liebsch, *Phys. Rev. B* **81**, 054513 (2010).
- [47] M. Aichhorn, L. Pourovskii, V. Vildosola, M. Ferrero, O. Parcollet, T. Miyake, A. Georges, S. Biermann, *Phys. Rev. B* **80**, 085101 (2009).
- [48] H. Q. Yuan, J. Singleton, F. F. Balakirev, S. A. Baily, G. F. Chen, J. L. Luo, N. L. Wang, *Nature* **457**, 565 (2009).
- [49] Y.-Z. Zhang, I. Opahle, H. O. Jeschke, and R. Valentí, *J. Phys.: Condensed Matter* **22**, 164208 (2010).
- [50] J.-H. Chu, J. G. Analytis, C. Kucharczyk, and I. R. Fisher, *Phys. Rev. B* **79**, 014506 (2009).
- [51] T. Moriya, K. Ueda, *Rep. Prog. Phys.* **66**, 1299 (2003).